Effect of Liquid Mixing on the Performance of Bubble Trays

ALAN S. FOSS, J. A. GERSTER, and R. L. PIGFORD

University of Delaware, Newark, Delaware

One of the major problems in the prediction and correlation of plate efficiencies for large trays is lack of knowledge of the gradient of liquid concentration from the tray inlet to the outlet. This gradient is a function of the amount of mixing of the liquid that occurs in the direction of liquid travel as the liquid flows across the tray. Heretofore, for lack of concrete information concerning liquid mixing, one has been forced to assume either that the liquid on the tray is completely mixed or that it is not mixed at all. These two assumptions often lead to serious inaccuracies in estimates of plate efficiency. The studies of liquid mixing reported in this paper were undertaken to establish the nature and extent of mixing and to develop calculational methods to account for its effect on plate efficiency.

In these studies the degree of liquid mixing was determined experimentally by a tracer technique of measuring the distribution of residence times of the liquid. Further, an expression relating the plate efficiency to these distribution functions has been derived. Plate efficiencies predicted by this relationship were checked by comparison with plate efficiencies measured under conditions for which the rate of liquid mixing and the point efficiency had been established quantitatively. A simplified calculation procedure is presented which affords a rapid means of computing plate efficiency under all mixing conditions.

HISTORICAL BACKGROUND

The first attempt to account quantitatively for the effect of liquid mixing on tray efficiency was made by Kirschbaum in 1934 (*14, 15*). He proposed that the tray be divided in the direction of liquid flow into several equal-sized, perfectly mixed pools and the liquid be imagined to flow from one pool into the next until it reached the outlet weir. A tray with a single pool corresponded to a perfectly mixed tray, and one with an infinite number of pools corresponded to an entirely unmixed tray (plug flow of liquid). Kirschbaum did not indicate, however, how to determine the number of pools.

In 1955 Gautreaux and O'Connell (*9*) revived the pool concept of Kirschbaum and derived an expression for the Murphree vapor efficiency E_{MV}, assuming that the equilibrium and operating lines were straight over the concentration range of a single tray. Their result was

$$E_{MV} = \lambda^{-1}\left[\left(1 + \frac{\lambda E_{OG}}{n}\right)^{n} - 1\right] \quad (1)$$

n being the number of pools, λ the ratio of the slopes of equilibrium and operating lines, and E_{OG} the point efficiency. A tentative correlation of the number of pools vs. tray length was presented.

A further extension of the pool concept has been developed by Marangozis and Johnson (*21*), who included the effect of a series of pools of perfectly mixed liquid in the vertical direction (direction of gas flow) as well as in the horizontal direction (direction of liquid flow).

Another approach to the problem of liquid mixing on distillation trays is based on the supposition that mixing takes place by an eddy-diffusion mechanism. In addition to material transport by the bulk flow of liquid across the tray, it is assumed that material is also transported from one position to another at a rate proportional to the concentration gradient in the direction of the liquid flow. By analogy to diffusion theory of the kinetic theory of gases, the proportionality factor is called an *eddy-diffusion coefficient.* Most of the activity in this field has been centered at the Massachusetts Institute of Technology. Several students working there under Gilliland have measured eddy-diffusion coefficients by a steady state tracer technique and then have utilized the measured values to correlate mass transfer results on both bubble-cap and sieve trays (*2, 3, 27, 30*).

Two recent investigations have employed still another mechanism. Oliver and Watson (*23*) and Warzel (*28*) have assumed that a certain fraction of the liquid at the exit weir is recircuited to the inlet weir, where it is mixed with the incoming liquid. This mechanism is not explicitly stated by Oliver and Watson but is by Warzel; the final expressions resulting from the two studies for the Murphree plate efficiency are identical. Both showed that the fractional mixing parameter increased with an increase in gas throughput. The fractional mixing parameter was calculated from the difference in the experimentally determined liquid concentration immediately preceding and immediately following the inlet weir.

APPROACH TO PROBLEM

The present approach to the problem differs from the studies just discussed. It is based on the supposition that mixing of the flowing liquid causes some of the liquid to reside on the tray for periods longer and/or shorter than the period of residence of some other portion of liquid. In other words, mixing of the liquid should produce an entire spectrum or distribution of liquid residence times capable of ranging all the way from zero to infinity. In the case of plug flow, all portions of the liquid reside on the tray for the same length of time, and in the case of perfect mixing a large portion of the liquid leaves the tray before the average liquid residence time has elapsed.

Actually, the use of the residence-time concept is quite old, dating back as far as 1894, when Stewart (*26*) determined flows in small blood vessels by measuring the time necessary for injected salt to flow from one point to another. It was not until 1953, however, that a unified and comprehensive treatment of the residence-time concept in continuous-flow systems appeared, when Danckwerts presented an outstanding paper on the subject (*4*) that detailed the fundamental ideas involved, along with applications to several types of processes being carried out in continuous-flow systems.

While Danckwerts was the first to present a generalized discussion on the topic, several previous workers had applied its principles in specific applications. MacMullin and Weber (*20*) discussed residence-time distributions of a series of continuous-flow–stirred-tank reactors. Gas residence times in a small fluidized bed were measured by Gilliland and Mason (*10*), and an attempt was made to compute from the known distribution and a known reaction-rate constant the degree of conversion of a reacting gas mixture flowing through the bed. More recently Danckwerts, Jenkins, and Place (*5*) injected a pulse of helium into the vapor stream entering a large-scale fluidized bed and measured the helium concentration in the effluent vapor to obtain residence-time distributions. Andersen and Matthias (*1*) used the distribution of residence times of catalyst particles in a fluidized bed to compute the steady state catalyst activity. A particularly interesting study is that of Jardine (*12*), who determined the residence-time distribution of gas bubbles

Alan S. Foss is with E. I. duPont de Nemours and Company, Inc., Wilmington, Delaware.

passing through the liquid on a sieve tray by a frequency-response technique. Other interesting applications and discussions of the residence-time concept appear in references noted by Danckwerts (*4*) and in other sources (*16, 22, 25, 31*).

Use of the residence-time concept to characterize the degree of liquid mixing on bubble trays appears to have few, if any, limitations in this application. The present approach is more realistic than the pool concept of Gautreaux and O'Connell or the fractional-liquid-mixing ideas of Warzel or of Oliver and Watson. It is unlikely that a number of well-mixed pools would actually exist on a bubble tray. The eddy-diffusion concept, of course, is merely an extension of the molecular-diffusion mechanism and is somewhat restricted in use; for example, it is incapable of describing extreme liquid by-passing and probably holds only when there are a large number of repetitions of the diffusive mechanism. The residence-time concept, on the other hand, should be able to describe all conditions.

EFFECT OF RESIDENCE-TIME DISTRIBUTION ON PLATE EFFICIENCY

A bubble tray operating normally with cross flow of liquid will be considered, with the liquid entering the tray assumed to consist of an infinite number of streams each of which is destined to reside on the tray a certain time. In one such stream the quantity of liquid may be denoted by

$L'f(t)\,dt$ = lb. moles/hour of liquid destined to have an age between t and $(t + dt)$ at the moment of leaving the tray

The function $f(t)$ here is the liquid residence-time function and in general would resemble the distribution function sketched in Figure 1. The mean or the first moment of this function is the mean residence time of the liquid, and the total area under the curve represents the sum of all fluid streams.

The concentration of dissolved material in each stream is affected by mass transfer to the gas at a constant local efficiency E_{OG}. The precise behavior of the liquid concentration of any given stream as it flows along the tray may be deduced by considering a material balance on a differential-volume element of that stream. If one assumes that the gas passes uniformly up through the liquid in plug flow and that the operating and equilibrium lines are straight for a given tray, one finds that the concentration of a given fluid stream at location ξ on the tray may be expressed as follows:

$$c(\xi, t) = c_{in}^* + (c_{in} - c_{in}^*) \exp(-\lambda E_{OG}\xi/\tau) \quad (2)$$

The mathematical details leading to this result are given in reference *7*.

By solving Equation (2) for the liquid concentrations at the tray exit ($\xi = 1$) and by weighting the concentration of each stream according to the residence-time distribution, one may compute the Murphree efficiencies. The expression for the Murphree vapor efficiency is

$$E_{MV} = \frac{1 - \int_0^\infty \exp(-\lambda E_{OG}t/\tau)f(t)\,dt}{\lambda \int_0^\infty \exp(-\lambda E_{OG}t/\tau)f(t)\,dt} \quad (3)$$

and the result for the Murphree liquid efficiency is

$$E_{ML} = \frac{1 - \int_0^\infty \exp(-\lambda E_{OG}t/\tau)f(t)\,dt}{1 - \lambda^{-1}\left[1 - \int_0^\infty \exp(-\lambda E_{OG}t/\tau)f(t)\,dt\right]} \quad (4)$$

Both these results reduce to the well-known expressions for efficiencies in the cases of no mixing (*19*) and complete mixing. It will be noticed that the integrals appearing in Equations (2) and (3) are in reality Laplace transformations of $f(t)$,

$$L\{f(t)\} = \int_0^\infty e^{-pt}f(t)\,dt \quad \text{with} \quad p = \lambda E_{OG}/\tau.$$

Thus it is possible to use a table of transforms to find E_{ML} and E_{MV} quickly when a functional form of $f(t)$ is given.

It is to be noted that the expressions for the Murphree plate efficiencies apply to all cases of liquid behavior, ranging from plug flow, where E_{MV} and E_{ML} are the highest, to the case of liquid by-passing, where the efficiencies drop below the point values and approach zero.

In order to check these relationships a comprehensive experimental program was undertaken. In the first set of experiments the liquid residence-time distribution function was measured, and in the second set, measurement was made of the point efficiency under the same operating conditions employed in the first. Use of these two sets of data in either Equation (3) or (4) permits a prediction to be made of the Murphree efficiency. These predicted Murphree efficiencies were then compared with experimental Murphree efficiencies determined in a third set of experiments.

EXPERIMENTS AND APPARATUS

Choice of Apparatus and Gas-liquid System

In the present work experiments were limited to sieve trays of constant hole diameter but varying total hole area and to one gas-liquid system. Sieve trays rather than bubble-cap trays were selected as the gas-liquid contacting device because of their simplicity. While bubble-cap trays are equally as important as gas-liquid contactors, it was felt that in this initial study, the fundamentals of the mixing process might best be studied where the flow of bubbling liquid was uncomplicated by the presence of bubble caps.

The system employed in these experiments was the desorption of oxygen-rich water with air. The tests were carried out at about 23°C. and total pressure of 1 atm. Since the solubility of oxygen in water is extremely low at these conditions, this system has only liquid-phase mass transfer resistance. To be sure, gas-phase controlling systems are equally important commercially, but the system chosen is entirely adequate for testing the hypothesis and does allow simplifications in the apparatus and experimental techniques.

In the present work the desire to simulate conditions of froth flow and behavior that might be expected in large-diameter commercial columns dictated the choice of a large experimental apparatus. It was felt, however, that authentic froth behavior could be obtained by considering only a slice down the center of a large tray between the inlet and outlet weirs. The tray then would be a rectangular one, and the width of the slice selected was 9.5 in. The length of liquid travel was the most important tray dimension, as the entire study was concerned with mixing in the direction of liquid flow. Preliminary tests indicated that a tray length of 36 in. would be enough to ensure tray behavior typical of the center of large-scale trays. The liquid flow at the periphery of circular trays is not accounted for in this apparatus; however on large trays this peripheral flow should be only a small portion of the total flow.

Some of the features of the apparatus included an outlet weir of variable height used to adjust the height of the froth, pressure taps connected to the tray floor for measurement of the height of clear liquid, liquid sampling taps along the tray, and provisions for dissolving oxygen into the water entering the tray unit. Changes in water temperature on the tray due to evaporation were eliminated by providing for the humidification of the entering air with small quantities of live steam. Also included was a section of tray to preaerate the incoming liquid in order to minimize end effects caused by the dumping of liquid onto the tray at the liquid inlet.

The preaeration section was used only at low gas throughputs and was separated from the 36-in. test section by a partitioning device constructed to allow the free flow of froth in the forward direction but to prevent back mixing past it. Various sieve trays could be installed easily into the apparatus, and these were fabricated by punching 3/16-in. holes on a triangular spacing into brass sheets 1/16 in. thick. The accompanying table summarizes the important dimensions of the trays used in this study.

Tray No.	Hole diameter, in.	Hole spacing, center-to-center, in.	% Free area of tray
1	3/16	7/8	4.16
4	3/16	5/8	8.0
2	3/16	17/32	10.6

Their over-all dimensions were 9.5 by 45 in. Further details concerning the tray unit may be obtained from reference 7.

Residence-time Experiments

The distribution of liquid residence times was measured by introducing a small amount of tracer material into the incoming liquid stream and monitoring the concentration of this tracer in the tray effluent with time. With this technique, it is implicitly assumed that a tracer particle behaves just as any other element of fluid and that the behavior of many elements of fluid may be determined by the behavior of the tracer material which represents these elements. As pointed out by Danckwerts (4), these assumptions may not hold if molecular diffusion of the tracer material is appreciable. In the present application, however, this effect would be undetectable experimentally.

If an instantaneous pulse of tracer material could be injected into the liquid just as it enters the tray, the time history of the tracer concentration at the exit weir would resemble the residence-time distribution function of Figure 1, and after the size of the input had been appropriately accounted for, it would be the actual liquid residence-time distribution. It is possible to obtain the same information by injecting a unit step input instead. Introduction of a sharp pulse input requires elaborate equipment, whereas rapid change of the inlet tracer concentration from one value to another is considerably less troublesome to achieve. This latter technique was used, and the response of the tray to this unit-step input gave directly the cumulative residence-time distribution. The residence-time distribution function itself was obtained from the cumulative distribution by differentiation with respect to time, a valid practice as the unit-pulse input is the derivative of the unit-step input. It must be assumed first, however, that the system, that is, the flowing froth containing the tracer, is linear and that therefore tracer concentrations must be additive, and this latter assumption is entirely reasonable.

The particular tracer material used was a concentrated solution of common salt in water. The main liquid supplied to the tray was tap water, and air from a blower passed upward through the single tray employed. Both air and water were at 23°C. and 1 atm. In order to produce a

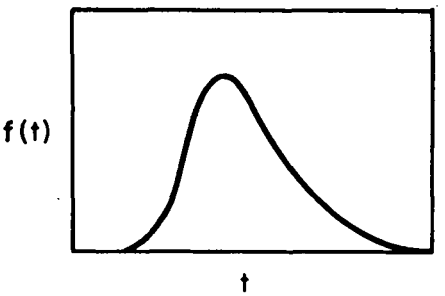

Fig. 1. Typical residence-time distribution function.

plane source of tracer at the liquid inlet, the salt solution was injected into the incoming liquid at several points closely spaced in both the vertical and transverse directions of the liquid cross section. This approximation of a plane source by a finite number of point sources distributed in a plane is satisfactory if the tracer from an individual point merges with tracer from surrounding points in a time which is short compared with the time required for the tracer to reach the concentration measuring element. Placing the point sources ½ in. apart in the present work assured the validity of such an approximation. The step input of salt tracer was achieved by instantaneously stopping the steady flow of the salt solution entering this distributing device. The rate at which salt solution was injected was usually about 1 or 2% of the main liquid flow rate. In all the experiments the salt concentration of the water never exceeded 0.1 wt. %.

The concentration history of salt in the liquid leaving the tray was determined by continuous measurement of the electrical conductivity of the liquid. A small conductivity cell which could be positioned at any point on the tray was constructed and operated so that it detected the instantaneous conductivity of the liquid. This cell acted as one arm of a Wheatstone's bridge, and the bridge unbalance at any instant was amplified and continuously recorded on a strip-chart recorder. Zero time was marked automatically on the strip chart at the instant the step input of salt occurred. Details of construction of the conductivity cell and of the device used to obtain a plane source of tracer are described fully in reference 7.

The design of an experimental program for the determination of the residence-time distribution was governed by preliminary scouting measurements. These preliminary runs led to selection of the following operating variables, which appeared to have the most important effect on the residence-time distribution.

Gas velocity	2 and 6 ft./sec.
Froth height	4 and 8 in.
Mean linear froth velocity	0.2 to 1.1 ft./sec. (run at three levels at each of the foregoing conditions)

The 4%-free-area tray was used for the 2 ft./sec. gas rate runs and the 11%-free-area tray for the 6 ft./sec. runs. This selection kept the gas velocity through the holes between 50 and 60 ft./sec.

Preliminary tests also showed that by measuring the distribution function at various points along the direction of liquid travel, one could follow its rate of spreading or its variance change with distance. The discovery that the variance increased linearly with distance immediately suggested the rate-of-increase-of-variance as a measure of the rate of mixing. Consequently the experimental program included measurement of the distribution function at six points along the 36-in.-long flow channel at each of the conditions tabulated above.

Plate Efficiency and Concentration Profile Experiments

Measurements of the liquid Murphree plate efficiencies and liquid concentration profiles were made under the same operating conditions as those employed in the residence-time experiments. Oxygen desorption from water into air was the system employed. At low froth velocities the tray length was shortened to 18 in. in order that oxygen would not be stripped entirely out of the liquid by the time it reached the end of the tray. Liquid samples taken at the liquid inlet and outlet and at various positions along the tray were analyzed for dissolved oxygen by the Winkler method. Experiments of this nature have been reported previously by the authors (8).

Liquid-phase Mass Transfer Coefficient Experiments

In order to predict the Murphree plate efficiency by Equation (3), it is necessary to know both the residence-time function and the point efficiency. For a liquid-phase controlling system, such as the oxygen-air-water system of this study, the (λE_{OG}) product in Equation (4) reduces to $N_L = (k_L a Z_f/L)$, the number of liquid-phase transfer units.

It was decided to measure $k_L a$ by a steady state method with a large pool of completely mixed froth. A large pool was desired so that the results obtained would truly be representative of mass transfer rates on large-scale trays. The pool was 6 in. wide and 24 in. long, and it had adjustable sides for control of the froth height. The sieve tray was the base of the pool. Oxygen-rich water was continuously fed to the pool, and froth spilled over the entire periphery of the boxlike pool enclosure. Ideally, in order to obtain a pool of uniform concentration, liquid should be introduced and removed at an infinite number of points, but this was approximated by introducing liquid at six equally spaced points on the long center line of the pool and allowing the liquid to leave at the pool edges. Liquid samples taken at several locations within the froth confirmed the constancy of the liquid composition throughout the pool. Under these conditions one may equate the rates of supply and removal of oxygen as follows:

$$L(c_{in} - c) = k_L a Z_f (c - \bar{c}_{out}^*) \qquad (5)$$

where c is the composition of the liquid on the tray (and also leaving the tray), and c_{in} is the composition of the entering liquid. The value of $k_L a$ was computed by use of experimentally measured values of oxygen concentration and froth height, Z_f.

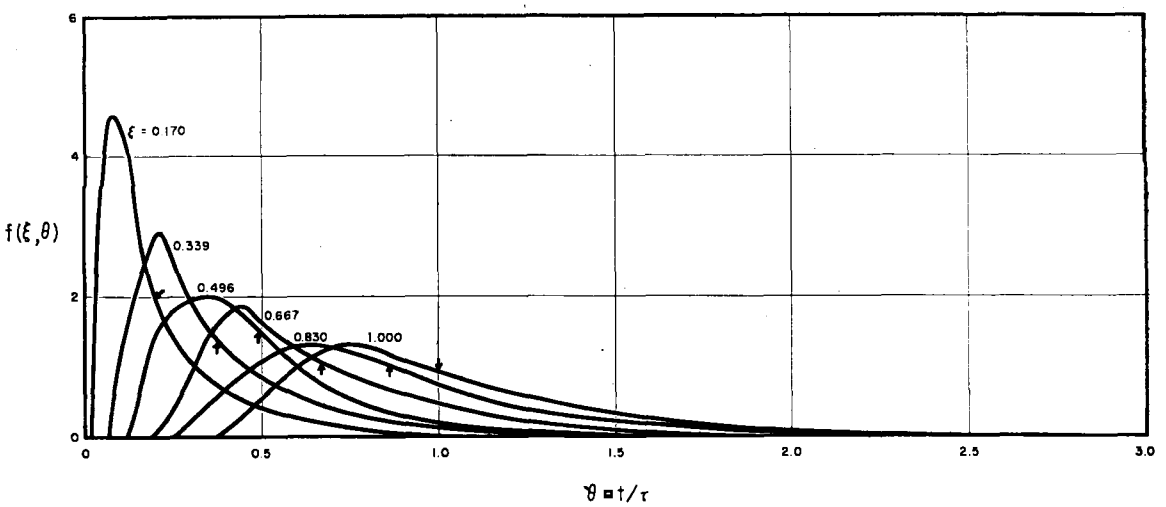

Fig. 2. Distribution of residence times of aerated water flowing across a 36-in.-long sieve tray at low froth velocity conditions. Mean residence time, τ, is 15.70 sec. Distribution function is shown as function of time, t, and fraction of total tray length, ξ. Arrows indicate mean liquid age at various positions, ξ. Gas velocity is 6.03 cu. ft./(sec.)(sq. ft. of bubbling area), liquid rate is 8.45 gal. (min.)(ft. tray width), froth height is 4.1 in., and froth velocity is 0.180 ft./sec. sieve tray has 10.6% free area.

RESIDENCE-TIME-DISTRIBUTION RESULTS

Residence-time distribution functions were determined from the strip-chart records by first averaging random concentration fluctuations in the four (sometimes three) replicate runs made at each condition. Averages were made visually at equally spaced values of time by superposition of the charts. These averaged strip-chart readings were then used to calculate the tray response to the unit-step input. The residence-time distribution function $f(t)$ was then computed from this by differentiation with respect to time by use of a 7-point–least-squares method (*24*).

Some typical distribution functions for high and low froth velocities are shown in Figures 2 and 3. The gas rate is 6 ft./sec., and the froth height is 4 in. for both runs. The time scale in these figures has been made dimensionless by dividing by the mean residence time τ. The distributions shown have been computed as a function of $\theta = t/\tau$. Complete data for these runs and runs at other operating conditions may be obtained from reference *7*. Note that the distributions at the high froth velocity are more sharply peaked than those at the lower velocity. At the high froth velocity no liquid leaves the tray until it has resided a time of at least one half the nominal residence time. At the low froth velocity liquid begins to leave somewhat earlier. In both cases only about 56% of the liquid has left the tray after residing one residence time. At high froth velocities only about 2.5% remains longer than 1.5 residence times, whereas 10.5% has ages greater than 1.5 at the low froth velocities. From these cursory observations, it may be stated only qualitatively at this point that the mixing rate at the low froth velocity appears somewhat higher than the rate at the higher velocity.

It is interesting to note also the position of the peaks relative to the means. A distribution that is peaked before the mean implies that there is some by-passing or short-circuiting of the liquid. Also, the distribution functions near the liquid inlet indicate some by-passing, but as one progresses along the tray, the distributions become more symmetrical and the peaks more nearly coincide with the means.

THE RATE OF LIQUID MIXING

One of the most significant findings of the present work was the linear increase of variance of the distribution function as it progressed along the tray. The constant rate-of-variance increase for a given operating condition was chosen as the function for characterizing the rate of liquid mixing for that condition. The variance measures dispersion, and the variance used here measures dispersions in the time domain rather than the space domain.

The variance $\sigma_t^2(w)$ of the distribution function $f(w, t')$ about its mean at w is defined as

$$\sigma^2(w) = \int_0^\infty (t' - t_1')^2 f(w, t')\, dt' \quad (6)$$

where t_1' is the mean or first moment of $f(w, t')$ and is defined as

$$t_1' = \int_0^\infty t' f(w, t')\, dt' \quad (7)$$

For a given run the variance of $f(w, t')$ was computed by numerical integration of Equation (6) at each of the six points on the tray and then plotted vs. its mean age t_1'. Figure 4 shows typical results for a high and low froth velocity. More correctly, the variance should have been plotted vs. tray position, and this would have been done had the six distribution functions for each operating condition been determined at precisely the same froth velocity. But since positioning of the cell at each of the six points required interruption of the flows between determinations of $f(w, t')$, the froth velocity varied slightly from the nominal value each time the flows were reset. By plotting in this manner, the effects of these small differences in froth velocity were absorbed in the variation of t_1' with froth velocity. A mean froth velocity was later assigned to the run so that the variance increase per foot of tray length might be determined.

The presence of nonuniform froth conditions at the ends of the tray may be noted on Figure 4. At high froth velocities the variances at the liquid inlet and outlet were so abnormal that the values of $\sigma_t^2(w)$ at those points could not be used to determine the slope of these lines. For this reason, also, there was no concern about obtaining negative intercepts since end effects could easily account for this. The linearity of the variance, then, holds only for the center of a large tray, but under certain conditions, such as low froth velocities, it may well hold for the entire tray.

In order to determine the time rate-of-variance increase for each operating condition, slopes of variance vs. t_1' plotted as in Figure 4 were computed by a least-squares procedure. This yielded a variance rate in sec.^{2}/sec., and in order to obtain the variance change per foot of tray length $d\sigma_t^2/dw$, the slopes of the lines of Figure 4 were divided by the froth velocity.

The values of the variance rates thus determined covered a wide range, depending upon such factors as froth velocity, froth height, gas rate, and liquid holdup. A convenient method of correlating these data has been developed and is given in Figure 5. In this figure the variance rate per unit of liquid holdup

$R_v \equiv (1/Z_c)\ (d\sigma_t^2/dw)$ has been plotted vs. froth momentum ϕV_f. According to Figure 5, the variance rate is uniquely determined by the liquid holdup and the froth momentum; gas rate and froth height are influencing factors only in the sense that they affect the holdup and momentum.

Froth momentum is believed to be one of the fundamental correlating variables because it affords some measure of the froth's tendency to remain in uniform motion. It is presumed that the higher the momentum of the froth flow, the more difficult it would be for any external force to change the velocity vector of a given froth element. The decrease in variance rate, then, with increased froth momentum is understandable.

Several authors have previously applied the eddy diffusion concept to mixing problems in continuous flow systems, and it is of interest to note the relation between the eddy-diffusion coefficient D and the rate of change of variance used in this work. Danckwerts (*4*) has shown that the eddy diffusion mechanism leads to the following cumulative distribution function at a point w on the tray:

$$F(w, t') = 1/2 \text{ erfc} \left[\frac{w - V_f t'}{2\sqrt{Dt'}}\right] \quad (8)$$

This relation holds only when the diffusion rate is small compared with the mass flow rate; that is, $D/(V_f w) \ll 1$. Using the derivative of Equation (7) to obtain the frequency function $f(w, t')$, one may then derive the relation between the variance and the eddy diffusion coefficient. (This derivation is available in reference 7.) The result is

$$\sigma_t^2 = \frac{1}{V_f}\left(\frac{2D}{V_f^2}\right)w \quad (9)$$

The rate of change of variance with distance is

$$\frac{d\sigma_t^2}{dw} = \frac{2D}{V_f^3} \quad (10)$$

Equation (9) states that the eddy-diffusion mechanism predicts a linear increase in variance with tray length, and this is precisely what has been found experimentally. Equation (10) gives directly the relation between the variance rate and eddy-diffusion coefficient, a relation that is surprisingly similar to the correlation of the mixing rate already presented in Figure 5. Data of Figure 5 indicate that R_v is proportional to the froth momentum ϕV_f raised to the -2.8 power. The similarity between this fact and the relation of Equation (9) should be noted. The empirical relation $R_v = 2.057 \times 10^{-3}\ (\phi V_f)^{-2.80}$ fits the data closely. R_v has units of (sec.²/ft.)/in., V_f is in ft./sec., and ϕ is dimensionless.

The correlation between the variance rate and froth momentum holds, of course, only as long as the variance rate is constant across the entire tray. For large-diameter trays one might assume without much error that this condition exists. In this case, an approximate distribution function can be obtained with knowledge of the variance rate. Use of this correlation, however, requires knowledge of the froth properties, and fortunately these are becoming more readily available. The froth characteristics of the trays used in this study have already been reported (*8*), and froth properties of several other systems on bubble-cap trays are being determined by the A.I.Ch.E. research program on plate efficiencies. Care should be exercised in using froth properties of other systems and other trays in the foregoing mixing-rate correlation, for there is no direct evidence that it will hold for other systems and other types of trays. The same general considerations should apply, however, to all systems and trays.

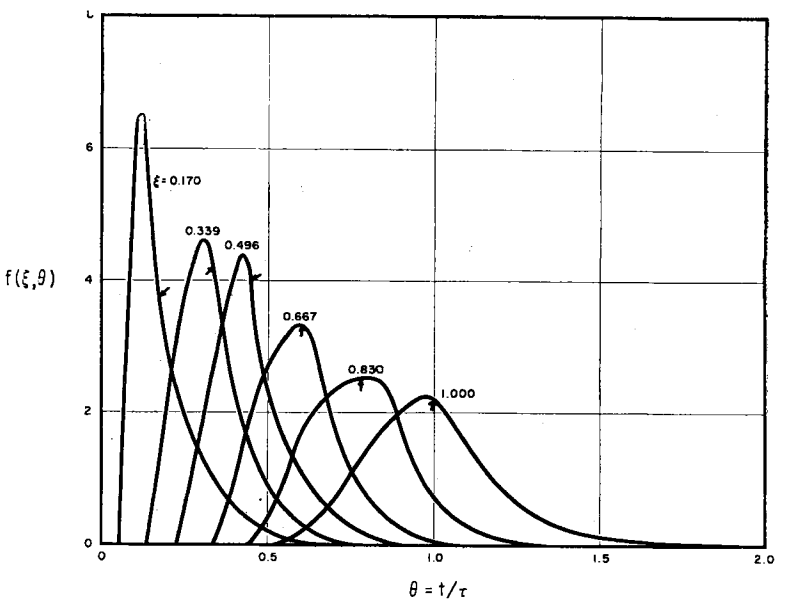

Fig. 3. Distribution of residence times of aerated water flowing across a 36 in.-long sieve tray at high froth velocity conditions. Mean residence time, τ, is 2.98 sec. Distribution function is shown as function of time, t, and fraction of total tray length, ξ. Arrows indicate mean liquid age at various positions, ξ. Gas velocity is 6.02 cu. ft./(sec.)(sq. ft. of bubbling area), liquid rate is 43.5 gal./ (min.)(ft. tray width), froth height is 4.0 in., and froth velocity is 1.08 ft./sec. Sieve tray has 10.6% free area.

RESULTS OF LIQUID-PHASE MASS TRANSFER COEFFICIENT STUDIES

Liquid-phase mass transfer coefficients were computed by Equation (5), measured oxygen concentrations being used in the thoroughly mixed pool previously described. The measured concentrations of dissolved oxygen at several points in the pool were not all precisely the same, but the variation was only slight, and an average of several determinations was used in the calculation of the k_La values. Values of the equilibrium concentration of dissolved oxygen $\bar{c}_{out}{}^*$ were calculated by use of the Henry's Law constant (*11*).

The liquid-phase mass transfer coefficient was found to be dependent on the two froth properties, froth density and froth height. The rate of liquid supply at any given froth height and froth density produced only a very slight variation in the k_La values, and these appeared to be random. The conclusion was that there was no effect of liquid rate and that k_La values could be correlated entirely as a function of froth height and froth density. Figure 6 shows the behavior of k_La with variation in both froth density and froth height. The froth-height parameter is the nominal value about which the froth height was controlled during the runs. Deviation from these values was usually not more than $\pm 1/4$ in. Detailed data are given in reference 7.

The solid lines on Figure 6 represent a least-squares fit of the data. Since froth density was allowed to vary as it pleased and since froth height could be controlled only approximately, use of the least-squares technique to correlate the effect of the froth properties on k_La seemed to be the most efficient way to treat the data. Furthermore, since values of k_La that obtained during the residence-time distribution runs were needed, a least-squares relation between k_La, Z_f, and ϕ was found to be particularly convenient in interpolating the experimental data to the given froth conditions. Initial examination of the data indicated that the factors that should be included in the regression model were linear terms in both ϕ and Z_f, a ϕZ_f interaction and a quadratic ϕ term. Determination of the coefficients led to the following result:

$$k_La = 1{,}197 - 3{,}478Z_f + 18{,}900\phi + 16{,}540\phi Z_f - 43{,}160\phi^2 \quad (11)$$

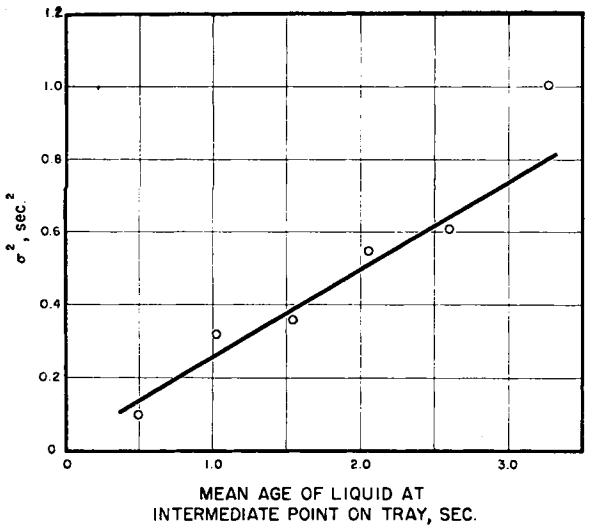

Fig. 4a. Increase of variance with mean age of liquid flowing across 36 in.-long sieve tray under high froth velocity conditions. Gas velocity is 6.04 cu. ft./(sec.)(sq. ft. of bubbling area). Liquid rate is 97.8 gal./(min.)(ft. tray width), froth height is 8.0 in., and froth velocity is 0.984 ft./sec. Sieve tray has 10.6% free area.

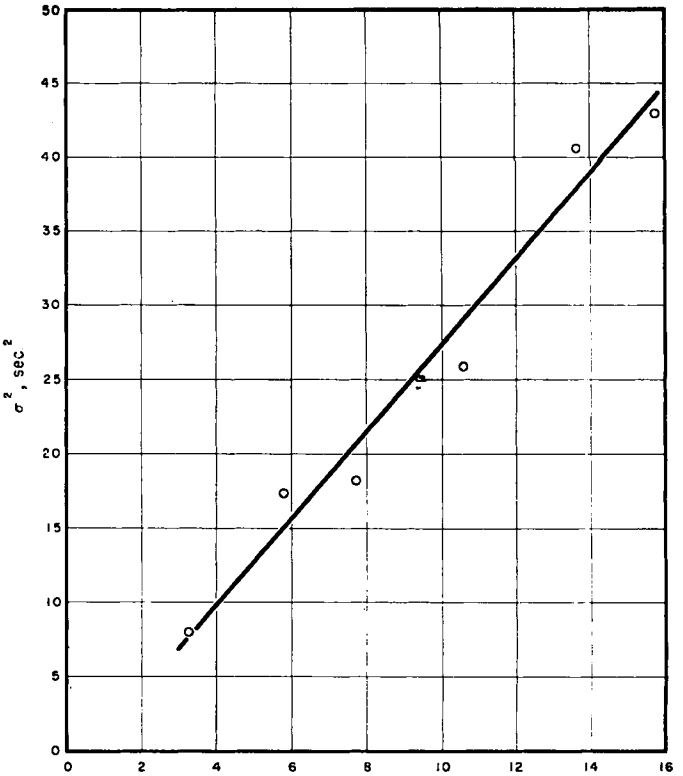

Fig. 4b. Increase of variance with mean age of liquid flowing across 36 in.-long sieve tray under low froth velocity conditions. Run conditions are same as in Fig. 2.

Equation (11) is shown as a series of solid lines on Figure 4. In the equation the units of k_La are pound-moles per hour per cubic feet of froth (unit mole fraction difference), Z_f is froth height in feet, and ϕ is froth density in cubic feet of clear liquid per cubic feet of froth. The water temperature averaged 21.1°C. The dotted lines about each froth-height line are 95% confidence limits; that is, the *a priori* probability is 0.95 that the least-squares-regression line will fall between the limits shown.

While these experiments have yielded significant findings concerning the behavior of mass transfer rates, they nevertheless represent a minor portion of the entire study. Unfortunately, space limitations prohibit a full interpretation of the results. It is believed, however, that the observed maximum of k_La is due almost entirely to changes in interfacial area with variation in froth density. The effect of increased froth height upon k_La is also of interest, and it is believed that changes in interfacial area with froth height also account for these effects. Several previous workers have reported sieve-tray behavior which supports both the trends and the absolute magnitude of the present results (*6, 8, 13, 17, 18, 29*).

CALCULATION OF PLATE EFFICIENCY AND CONCENTRATION PROFILES FROM RESIDENCE-TIME DATA

After determination of both the residence-time distribution for a given operating condition and the mass transfer coefficient applicable at that condition, it is now possible to compute the actual tray efficiency by Equation (4). For the case of a liquid-phase controlling system, Equation (4) reduces to

$$E_{ML} = 1 - \int_0^\infty e^{-N_L t/\tau} f(t)\, dt = 1 - \int_0^1 e^{-N_L t/\tau}\, dF(t) \qquad (12)$$

It should be remembered that in this expression $N_L = k_La(Z_f/L)$.

It is also possible to compute the oxygen concentration profiles along the tray by making use of the distribution functions $f(\xi, t')$ that were also measured. The question arises, however, as to the precise definition of the distribution function measured at an intermediate point on the tray. It is supposed that the conductivity cell without discrimination samples all fluid "particles" within a small slice of froth in which the cell is located. Or, alternately, one may state that all "particles" of fluid in this small slice of froth have equal probabilities of entering the cell. However, the number of "particles" entering the cell belonging to a given time group contained in the slice would be proportional to the fraction of the slice volume occupied by this group. The cell, then, measures a volume- or space-average salt concentration. The measured distribution function $f(\xi, t')\, dt'$, therefore, may be defined as the fraction of the fluid contained in a small slice at ξ that has an age ranging between t' and $(t' + dt')$.

The distribution functions may then be used in conjunction with Equation (2) to compute the concentration at any point ξ:

$$\frac{c(\xi) - c_{in}^*}{c_{in} - c_{in}^*} = \int_0^\infty e^{-N_L t'/\tau} f(\xi, t')\, dt' = \int_0^1 e^{-N_L t'/\tau}\, dF(\xi, t') \qquad (13)$$

where

t' = age of fluid stream at point ξ on tray = ξt

t = age of fluid stream at moment of leaving the tray

As both ϕ and Z_f were measured experimentally, the value of k_La could be estimated by the previously determined least-squares equation (11). Integration was carried out numerically by use of Simpson's rule. A typical concentration profile calculated in this manner is shown in Figure 7. For comparison, the concentration profile of oxygen measured under conditions identical to those of the residence-time distribution run is also plotted here, and the concentration profile for no mixing is indicated also. For all conditions studied, the calculated profiles always fell below the experimentally determined profiles, an indication that the predicted rates of mass transfer were too high. Detailed con-

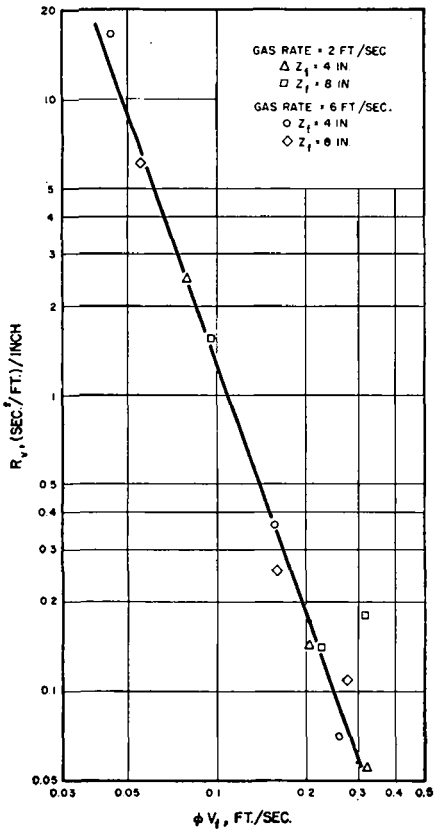

Fig. 5. General correlation of liquid mixing results, R_v, the rate of increase of variance with tray length (sec.²/ft.)/in. liquid holdup on the tray is correlated with the product of ϕ, froth density (cu. ft. of liquid holdup/sq. ft. of bubbling area/cu. ft. of froth/sq. ft. of bubbling area) and V_f, froth velocity (ft./sec.). Data are shown for two values of gas rate and for two values of froth height, Z_f.

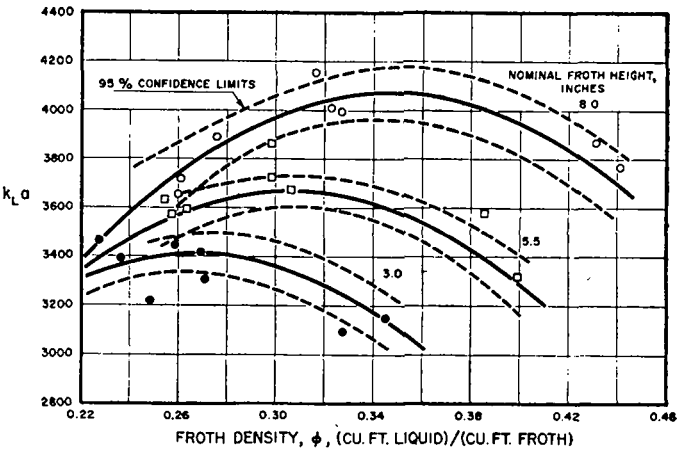

Fig. 6. Experimental values of liquid-phase mass transfer coefficient, k_La, for the desorption of oxygen from oxygen-rich water by air at 21°C. on a sieve tray. The units of k_La are lb. moles/(hr.)(cu. ft. froth) (unit mole fraction difference). Correlating variables are froth density and froth height.

centration-profile data for all runs are available from reference 7. Unfortunately, most of the liquid-phase efficiencies ranged between 90 and 100%, and experimental and calculated values of E_{ML} were too close for a fair comparison. For this reason, the experimental and calculated profiles afford the best means of comparison, particularly when they are represented on semilogarithmic coordinates as in Figure 8. For the case of no mixing, it is known that such a plot yields a straight line with an intercept at 1.0, and for a liquid-phase controlling system, a slope equal to $-N_L$. For complete mixing the slope is zero. When the liquid is only partially mixed, it is not immediately evident that the log profile should be straight, but if it were, its slope would lie somewhere between $-N_L$ and zero. Figure 8 shows a typical plot of experimental and calculated profiles. The linearity of this semilog plot has been found previously in experiments by Stone (*27*).

Figure 8 shows the zero intercept greater than 1.0. It is not possible, of course, for liquid on the tray to have a concentration greater than the inlet concentration, and to have an intercept of even 1.0 is unrealistic. As liquid mixing at the inlet immediately dilutes the incoming liquid, the concentration at that point is always less than the incoming liquid concentration. This fact has been verified experimentally in this work. This means that the straight-line relationship of Figure 8 does not hold in the region close to the liquid inlet, apparently because of nonuniform froth conditions at that point. No attempt was made, therefore, to extrapolate the concentration profiles to the liquid entrance.

The nonuniformity of the froth at the inlet is most likely the reason for the discrepancy between the calculated and experimental profiles. The experimental profiles seem to indicate that the first few inches of the tray are ineffective. In calculating the profiles by Equation (13), however, a constant value of k_La was used for the entire tray. To compare properly the calculated and experimental profiles, only the portion of the tray in which the k_La value is constant should be considered. The zero-distance coordinate would begin at some point downstream from the inlet and the net result would be a shifting to the left of the experimental profile.

There still remains the possibility that the k_La values are slightly in error. This might arise had there been a small amount of nonmixing of liquid in the pool experiments. Only a slight variation from the fully mixed case will result in large discrepancies in the calculated values of k_La.

Approximate Calculation of Plate Efficiency

Calculation of the plate efficiency by Equations (3) and (4) requires detailed knowledge of the distribution function, and if this information is in tabular or graphical form, the calculation becomes tedious. Considerable simplification results by employing an approximate analytical representation of the distribution function. Relating the parameters of this approximate distribution function to the variance rates correlated in Figure 5 gives a rapid method for estimating plate efficiency.

A function which appears to fit the measured residence times reasonably well is of the form

$$f(\theta) = \alpha\theta^{\beta}e^{\gamma\theta} \qquad (14)$$

Equating the first and second moments of this function to unity and σ^2 respectively shows that

$$f(\theta) = \frac{\theta^b e^{-\theta/\sigma^2}}{b!\sigma^{2(b+1)}} \qquad (15)$$

where b is defined as $1/\sigma^2 - 1$. This function may be substituted into Equations (3) and (4) and the integrations performed analytically. For the case of liquid phase controlling mass transfer resistance,

$$E_{ML} = 1 - (1 + N_L\sigma^2)^{-1/\sigma^2} \qquad (16)$$

E_{ML} may now be calculated from knowledge of the variance at the tray exit and the value of N_L.

A surprising result of this approximation is that the derived expression for the Murphree efficiency is the same as that given by the pool concept. The value of $1/\sigma^2$ in Equation (16) above corresponds to n, the number of pools in Equation (1). This correspondence should not be taken to mean that the present work substantiates the presence of pools. Use of an empirical equation different from Equation (14) would probably represent the experimental distribution functions equally as well, but would not lead to a final equation identical in form to the pool equation. Agreement between the form of the final equation with that of the pool equation must be considered as fortuitous. In this same regard, MacMullin in a review of this paper has suggested that the measured distribution functions be compared with those which he derived for a series of n stirred tanks (*20*). The value of n estimated by this visual comparison might then be used in the equation of Gautreaux and O'Connell (*9*) to calculate the Murphree efficiency.

The relation between E_{ML} and the variance as given by Equation (16) now makes prediction of the plate efficiency

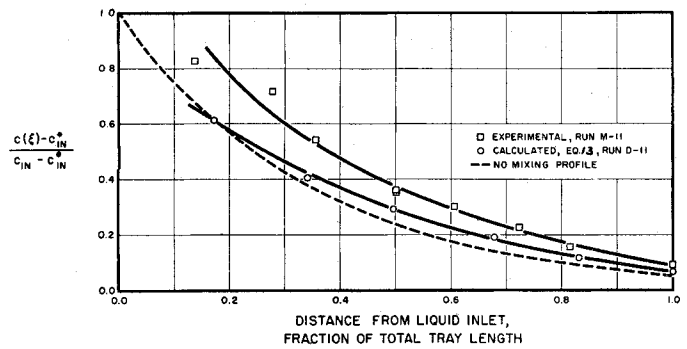

Fig. 7. Comparison of experimental liquid concentrations on active sieve tray as function of distance, ξ, with liquid concentrations predicted by Eq. (13). Dashed line shows predicted liquid concentration profile in absence of liquid mixing (*19*). System is desorption of oxygen from oxygen-rich water with air at 21°C. Gas velocity is 6.01 cu. ft./(sec.)(sq. ft. bubbling area), liquid velocity is 27.0 gal./(min.)(ft. tray width), froth height is 4.06 in., and froth velocity is 0.663 ft./sec. Sieve tray is 36 in. long and has 10.6% free area.

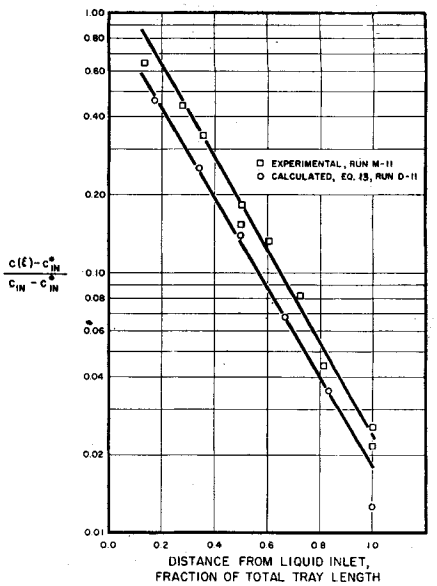

Fig. 8. Same plot as Fig. 7 but on semi-logarithmic coordinates.

fairly simple. A sample calculation is given below to illustrate the method of predicting the plate efficiency from knowledge of the column conditions.

EXAMPLE

Estimate the Murphree efficiency to be obtained on a sieve-tray unit on which oxygen is being stripped from oxygen-rich water with air under conditions identical to those reported in run 22*a* by Foss and Gerster (*8*). The experimental efficiency reported in (*8*) was 71.0% and the run conditions were as follows:

Liquid rate	= 50 gal./(min.)(ft. weir)
Gas rate	= 6.48 cu. ft./(sec.)(sq. ft. bubbling area)
Froth height	= 7.4 in.
Froth density	= 0.154 cu. ft. liquid/cu. ft. froth
Water temperature	= 22.2°C.
Tray length	= 1.5 ft.

Substitution of the known froth height and froth density values into Equation (11) gives a value of k_La = 2,511 lb.-moles/(hr.)(cu. ft.). This value applies at a temperature of 21.1°C., at which the point-efficiency measurements were made; it must now be corrected to the temperature of interest, 22.2°C. The correction factor, which is the square root of the ratio of the dimensionless Schmidt number at 22.2°C. to the Schmidt number at 21.1°C., is only 0.995, but the method is given as a matter of general interest. Thus at 22.2°C., k_La = 0.995(2511) = 2,497. The value of N_L then becomes

$$N_L = k_La Z_f/L$$

$$= \left[\frac{2{,}497(7.4/12)}{50}\right]\left[\frac{(18)(1.5)}{(8.33)(60)}\right]$$

$$= 1.663$$

The factors in the right-hand bracket convert the liquid rate to pound-moles/(hour) (square feet of tray area).

The variance is obtained from Figure 5 from knowledge of the froth momentum. If Q is the clear liquid rate, cu. ft./(sec.)(ft. of weir), then the froth velocity V_f is $(Q/\phi)/Z_f$ ft./sec., and the froth momentum ϕV_f is Q/Z_f ft./sec. In the present instance,

$$\phi V_f = \left[\frac{50}{(7.48)(60)}\right]\left[\frac{1}{(7.4/12)}\right]$$

$$= 0.181 \text{ ft./sec.}$$

From Figure 5 the corresponding value of R_v or $(d\sigma_t^2/dw)\,Z_c$ is 0.247 (sec.²/ft.)/in., and

$$\sigma_t^2 = Z_c W \frac{d\sigma^2}{dw}$$

$$= [(7.4)(0.154)](1.5)(0.247)$$

$$= 0.423 \text{ sec.}^2$$

The mean liquid residence time is

$$\tau = (Z_c W)/Q$$

$$= \left[\frac{(7.4)(0.154)}{12}\right](1.5)\left[\frac{(7.48)(60)}{50}\right]$$

$$= 1.279 \text{ sec.}$$

and so

$$1/\sigma^2 = n = \tau^2/\sigma_t^2$$

$$= 1.279^2/0.423 = 3.869$$

from which the Murphree efficiency may be predicted by Equation (16):

$$E_{ML} = 1 - (1 + N_L\sigma^2)^{-1/\sigma^2}$$

$$= 1 - (1 + 1.663/3.869)^{-3.869}$$

$$= 0.749 \quad \text{or} \quad 74.9\%$$

The experimental value of 71.0% is again somewhat less than the predicted value of 74.9%. Had the liquid been completely mixed, E_{ML} would have been 62.4%, and had it been not mixed at all, E_{ML} would have been 81.0%.

Estimated E_{ML} values for the other runs of Foss and Gerster (*8*) indicate that this technique does a fairly good job of prediction when the gas rate is high and liquid rate is low. These conditions usually lead to considerable mixing (small values of $n = 1/\sigma^2$). In all cases, however, the estimate is high. At low gas rates (2–4 ft./sec.), the predicted E_{ML} values do not check at all well with measured efficiencies, the predicted values being again too high. These differences might be attributed to the approximation technique or errors in the k_La values, but it is more likely that they result from nonuniform conditions in the froth at the liquid entrance. There is no way at present to estimate the mass transfer coefficient in this region, nor are there data to indicate the effect on the residence-time distribution function. It appears that these conditions must be taken into account by subtracting an "ineffective" length from the actual distance of liquid travel. Corrections of this nature have been employed by Stone (*27*), who found that they may amount to as much as 5 in. of tray length.

SUMMARY

Liquid flowing across a distillation tray seldom, if ever, travels from inlet to outlet without mixing in the longitudinal direction. Usually the mixing is incomplete and a concentration gradient exists in the liquid phase. Mixing of the liquid causes some liquid to reside on the tray for periods longer and/or shorter than the time of residence of other portions of liquid. It is found that the plate efficiency is greatly altered by the distribution of liquid residence times thus produced, and the relationship between these two has been derived.

In order to check the derived relations, residence-time distributions for several operating conditions were determined experimentally. By use of these residence-time distributions in conjunction with measured values of the mass transfer coefficient, efficiencies and liquid concentration profiles were computed and compared with actual experimental profiles and efficiencies. The predicted mass transfer rates were somewhat high.

In addition, the rate of mixing has been characterized by the rate of increase of variance of the ages of fluid elements as they flowed across the tray. This measure of the rate of dispersion within the froth was found to depend only on the bulk momentum of the flowing froth and the liquid holdup per unit tray area. Gas rate and height of the froth had no effect on the rate of mixing separate and distinct from their effect upon the liquid holdup and froth momentum. A method has been developed whereby this correlation of mixing rates may be used to predict rapidly the plate efficiency when liquid mixing occurs.

ACKNOWLEDGMENT

This investigation was made possible by fellowship grants from the E. I. du Pont de Nemours and Company, Inc., Wilmington, Delaware, and the Ethyl Corporation, Detroit, Michigan. Use of the computing facilities of the du Pont Engineering Department during the early stages of this work is sincerely appreciated.

NOTATION

c = mole fraction of volatile component in liquid at a given point on tray

$c(\xi, t)$ = mole fraction of volatile component in liquid element at point ξ which is to reside on the tray for a time between t and $(t + dt)$

c_{in} = mole fraction of volatile component in liquid entering tray

c^*_{in} = mole fraction of volatile component in liquid that would be in equilibrium with entering gas

$\bar{c}^*_{out}$ = mole fraction of volatile component in liquid which would be in equilibrium with the average composition of the gas leaving tray

D = eddy-diffusion coefficient, sq. ft./sec.

E_{OG} = Murphree vapor point efficiency $= \dfrac{y - y_{in}}{y^* - y_{in}}$

E_{MV} = Murphree vapor plate efficiency $= \dfrac{\bar{y} - y_{in}}{y_{out}^* - y_{in}}$

E_{ML} = Murphree liquid plate efficiency $= \dfrac{c_{in} - c}{c_{in} - \bar{c}_{out}^*}$

$f(t)\,dt$ = fraction of the liquid flow which has ages between t and $(t + dt)$ at instant of leaving tray

$F(t)$ = cumulative residence-time distribution function $= \int_0^t f(x)\,dx$

G = molar gas rate, lb.-mole/(hr.)(sq. ft.)

k_La = liquid-phase mass transfer coefficient, lb.-mole/(hr.)(cu. ft. froth)(unit mole fraction difference)

L = molar liquid rate, lb.-mole/(hr.)(sq. ft.)

L' = molar liquid rate, lb.-mole/hr.

m = slope of equilibrium line

n = number of hypothetical completely mixed pools or stirred tanks

N_L = number of liquid-phase transfer units

Q = clear liquid rate, cu. ft./(sec.)(ft. of weir)

$R_v = \dfrac{1}{Z_c}\dfrac{d\sigma_t^2}{dw}$, rate of increase of variance, Z_c in in., σ_t in sec., w in ft.

t, t' = time, sec.

t_1, t_2 = first and second moments respectively of the distribution function $f(w, t)$

V_f = mean linear froth velocity, ft./sec.

w = horizontal distance along aerated portion of tray up to point in question; measured from liquid inlet of test section, ft.

W = total horizontal distance between liquid inlet and outlet of test section, ft.

y = mole fraction of volatile component in gas which has just left a given point on the tray

y_{in} = mole fraction of volatile component in gas entering tray, assumed constant for entire tray

$\bar{y}$ = average mole fraction of volatile component in mixed gas leaving entire tray

y^*_{out} = mole fraction of volatile component in gas which would be in equilibrium with liquid leaving tray

y^* = mole fraction of volatile component in gas in equilibrium with liquid at a given point on tray

Z_c = height of clear liquid on operating tray

Z_f = height of aerated liquid above tray floor, ft.

α, β, γ = constants

θ = t/τ, dimensionless time

λ = (mG/L)

ξ = w/W, dimensionless distance

$\sigma_t^2(w)$ = variance of ages of fluid elements at point w, $(\text{sec.})^2$, computed as $t_2 - (t_1)^2$

$\sigma^2(w)$ = dimensionless variance $= \dfrac{\sigma_t^2(w)}{\tau^2}$

τ = mean age of fluid elements leaving tray, sec.

ϕ = froth density, computed as Z_c/Z_f, (cu. ft. clear liquid)/(cu. ft. froth)

$\operatorname{erfc}(x)$ = complementary error function $= \dfrac{2}{\sqrt{\pi}}\int_x^\infty e^{-u^2}\,du$

LITERATURE CITED

1. Andersen, S. L., and R. H. Matthias, *Ind. Eng. Chem.* **46**, 1296 (1954).
2. Anderson, J. E., Dr. S. thesis, Mass. Inst. Technol., Cambridge (1954).
3. Brown, J. W., Jr., B.S. thesis, Mass. Inst. Technol., Cambridge (1954).
4. Danckwerts, P. V., *Chem. Eng. Sci.*, **2**, 1 (1953).
5. ———, J. W. Jenkins, and G. Place, *ibid.*, **3**, 26 (1954).
6. Dixon, B. E., and P. R. Kiff, *J. Appl. Chem. (London)*, **5**, 390 (1955).
7. Foss, A. S., Ph.D. thesis, Univ. of Delaware, Newark (1957).
8. ———, and J. A. Gerster, *Chem. Eng. Progr.*, **52**, 28J (1956).
9. Gautreaux, M. F. and H. E. O'Connell, *ibid.*, **51**, 232 (1955).
10. Gilliland, E. R., and E. A. Mason, *Ind. Eng. Chem.*, **44**, 218 (1952).
11. "International Critical Tables," vol. 3, p. 257, McGraw-Hill Book Company, Inc., New York (1929).
12. Jardine, D. A., Ph.D. thesis, Univ. of Delaware, Newark (1957).
13. Kamei, S., T. Takamatsu, and K. Yamada, *Chem. Eng. (Japan)*, **18**, 467 (1954).
14. Kirschbaum, E., *Forsch. Gebiete Ingenieurw.*, **B5**, 245 (1935).
15. ———, "Distillation and Rectification," p. 276, Chemical Publishing Company, New York (1948).
16. Kramers, H., and G. Alberda, *Chem. Eng. Sci.*, **2**, 173 (1953).
17. Kuzminykh, I. N., L. S. Aksel'rod, Z. A. Koval, and A. I. Rodionov, *Khim. Prom.*, p. 86 (1954).
18. Kuzminykh, I. N. and Z. A. Koval, *J. Appl. Chem. (U.S.S.R.)*, **28**, 17 (1955) (English translation).
19. Lewis, W. K., Jr., *Ind. Eng. Chem.*, **28**, 399 (1936).
20. MacMullin, R. B., and M. Weber, Jr., *Trans., A.I.Ch.E.*, **31**, 409 (1935).
21. Marangozis, J. and A. I. Johnson, "The Use of a Digital Computer for Mixing Calculations in Distillation-tray Calculations," Univ. of Toronto (1956), unpublished.
22. Miskell, F., and W. R. Marshall, Jr., *Chem. Eng. Progr.*, **52**, 35J (1956).
23. Oliver, E. D., and C. C. Watson, *A.I.Ch.E. Journal*, **2**, 18 (1956).
24. Sherwood, T. K., and C. E. Reed, "Applied Mathematics in Chemical Engineering," p. 287, McGraw-Hill Book Company, Inc., New York (1939).
25. Sherwood, T. K., *Chem. Eng. Progr.*, **51**, 303 (1955).
26. Stewart, G. N., *J. Physiol.*, **15**, 1 (1894).
27. Stone, H. L., Dr. S. thesis, Mass. Inst. Technol., Cambridge (1953).
28. Warzel, L., Ph.D. thesis, Univ. of Michigan, Ann Arbor (1955).
29. West, F. B., W. D. Gilbert, and T. Shimizu, *Ind. Eng. Chem.*, **44**, 2470 (1952).
30. Wharton, L., B.S. thesis, Mass. Inst. Technol., Cambridge (1955).
31. Yagi, S., and T. Miyanchi, *Chem. Eng. (Japan)*, **17**, 382 (1953); **19**, 507 (1955).

Manuscript received Aug. 8, 1956; revision received Jan. 2, 1958; paper accepted Jan. 23, 1958.